doi:10.1093/jmcb/mjv017
Published online March 16, 2015

Article

Network-based identification of feedback modules that control RhoA activity and cell migration

Tae-Hwan Kim[1,†], Naser Monsefi[2,†], Je-Hoon Song[1], Alex von Kriegsheim[2], Drieke Vandamme[2], Olivier Pertz[3], Boris N. Kholodenko[2,4,5], Walter Kolch[2,4,5,*], and Kwang-Hyun Cho[1,*]

[1] Department of Bio and Brain Engineering, Korea Advanced Institute of Science and Technology (KAIST), Daejeon 305-701, Republic of Korea
[2] Systems Biology Ireland, University College Dublin, Belfield, Dublin 4, Ireland
[3] Department of Biomedicine, University of Basel, Basel, Switzerland
[4] School of Medicine and Medical Science, University College Dublin, Belfield, Dublin 4, Ireland
[5] Conway Institute of Biomolecular & Biomedical Research, University College Dublin, Belfield, Dublin 4, Ireland
[†] These authors contributed equally to this work.
[*] Correspondence to: Kwang-Hyun Cho, E-mail: ckh@kaist.ac.kr; Walter Kolch, E-mail: walter.kolch@ucd.ie

Cancer cell migration enables metastatic spread causing most cancer deaths. Rho-family GTPases control cell migration, but being embedded in a highly interconnected feedback network, the control of their dynamical behavior during cell migration remains elusive. To address this question, we reconstructed the Rho-family GTPases signaling network involved in cell migration, and developed a Boolean network model to analyze the different states and emergent rewiring of the Rho-family GTPases signaling network at protrusions and during extracellular matrix-dependent cell migration. Extensive simulations and experimental validations revealed that the bursts of RhoA activity induced at protrusions by EGF are regulated by a negative-feedback module composed of Src, FAK, and CSK. Interestingly, perturbing this module interfered with cyclic Rho activation and extracellular matrix-dependent migration, suggesting that CSK inhibition can be a novel and effective intervention strategy for blocking extracellular matrix-dependent cancer cell migration, while Src inhibition might fail, depending on the genetic background of cells. Thus, this study provides new insights into the mechanisms that regulate the intricate activation states of Rho-family GTPases during extracellular matrix-dependent migration, revealing potential new targets for interfering with extracellular matrix-dependent cancer cell migration.

Keywords: cell migration, Rho-family GTPases, signaling network, Boolean network model, cyclical RhoA bursts

Introduction

Cell migration is a complex process controlled by various extracellular matrix (ECM) and cellular determinants that are cell-type dependent (Friedl and Wolf, 2010). For some cell types such as leukocytes, migration is essential for their immune-defensive function, and hence maintained throughout their life span (Friedl and Wolf, 2010). For most cell types, however, migration is strictly confined to morphogenesis during development except for tissue regeneration or neoplasia (Friedl and Wolf, 2010). Cancer cells often escape from this strict regulation of migration and metastasize to form secondary tumors away from the primary tumor, causing most cancer deaths (Hanahan and Weinberg, 2000; Croft and Olson, 2008).

Several lines of evidence have highlighted the pivotal role of Rho-family GTPases that work together to control cytoskeleton dynamics in the process of cell migration (Sahai and Marshall, 2002; Machacek et al., 2009). Members of the Rho-family, which include RhoA, Rac1, and Cdc42, are critical for cell migration, and their activities need to be tightly coordinated in order to allow cells to move (Heasman and Ridley, 2008). RhoA has been involved in regulating both leading edge membrane protrusion (Pertz et al., 2006; Machacek et al., 2009) and the contractile force for moving the body and tail of the cell (Sahai and Marshall, 2002). Rac1 induces the assembly of actin-rich lamellipodia at the leading edge of the cell. Cdc42 is thought to be involved in establishing the directionality of movement by forming actin-rich spikes (filopodia) that can sense chemotactic signals (Sahai and Marshall, 2002). Consistently, studies with FRET-based biosensors have shown that all three GTPases are activated at the leading edge (Machacek et al., 2009), while RhoA activity has also been observed at the trailing edge (Pertz et al., 2006). Furthermore, RhoA, Rac1, and Cdc42 can mutually regulate each other's activities (Sander et al., 1999; Burridge and Wennerberg, 2004; Sanz-Moreno et al., 2008; Machacek et al., 2009; Friedl and Wolf, 2010; Tsyganov et al., 2012).

Received August 12, 2014. Revised December 9, 2014. Accepted December 25, 2014.
© The Author (2015). Published by Oxford University Press on behalf of *Journal of Molecular Cell Biology*, IBCB, SIBS, CAS. All rights reserved.

Downloaded from https://academic.oup.com/jmcb/article/7/3/242/890313 by guest on 20 August 2022

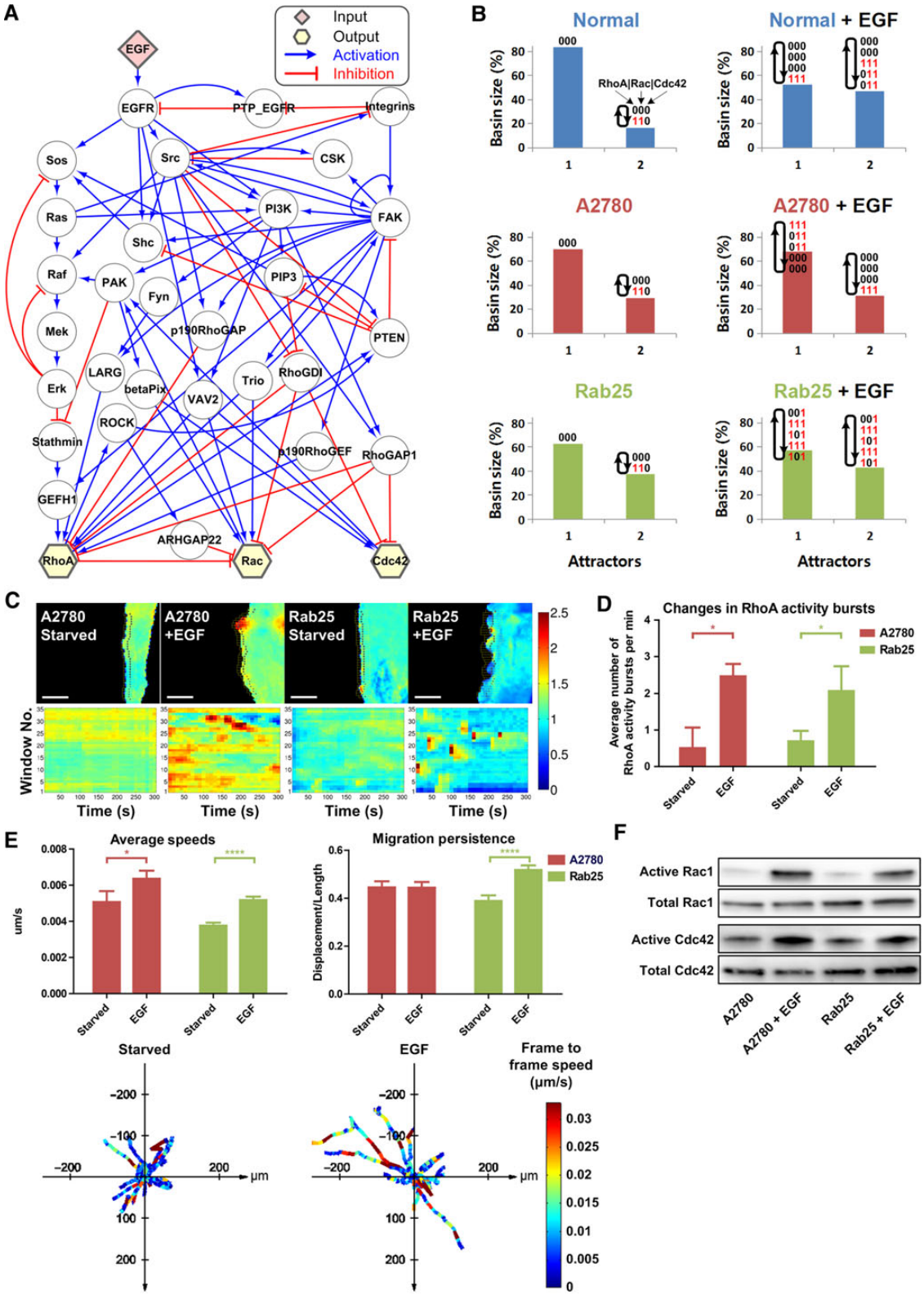

Figure 1 Steady-state dynamics of the Rho-family GTPases signaling network. (**A**) The reconstructed Rho-family GTPases signaling network consisting of 33 nodes and 83 directed links, in which 60 links are activating (arrows) and 23 are inhibiting (blunted arrows). The network is highly interconnected with at least 121 (62 negative and 59 positive) feedback loops (Supplementary Table S3). More mechanistic details about each link and the assigned logic table for each node are described in Supplementary Tables S1 and S3, respectively. (**B**) Steady-state dynamics of the attractors. The attractors were identified from Boolean simulations using 1000000 initial network states (see Supplementary Materials and

Downloaded from https://academic.oup.com/jmcb/article/7/3/242/890313 by guest on 20 August 2022

A number of reports indicate that the coordinated cyclic iteration of leading edge protrusion and subsequent rear end retraction is required for cell movement (Lauffenburger and Horwitz, 1996; Lammermann and Sixt, 2009; Friedl and Wolf, 2010). Moreover, it has been suggested that the occurrence of high RhoA and Rac activities at the leading edge is likely cyclic, thereby providing a necessary push-pull mechanism for cell migration (Tomar and Schlaepfer, 2009). Another layer of regulation is the interface between the forces that regulate actin polymerization and depolymerization at protrusions and the signal transduction events that stimulate cell migration. Recent results suggest that actin polymerization and depolymerization occur in cycles and that signaling events impinge on these cycles and stabilize protrusions to enable migration (Huang et al., 2013).

Many reports showing their aberrant regulation in various tumor types suggest the Rho-family GTPases as putative therapeutic targets for inhibiting metastasis (Sahai and Marshall, 2002). However, accumulating evidence indicates that they are embedded in a highly interconnected feedback network that intricately regulates their activities (Figure 1A). Thus, the mechanisms by which Rho-family GTPases are regulated and especially how their activities are coordinated to promote cell migration are still poorly understood. This raises intriguing questions: (i) what determines the cyclic behavior of Rho-family GTPases at the leading edge that enables cell migration; and (ii) which component should be targeted in the context of a complex signaling network to effectively block the cancer cell migration?

Here, we investigated these questions by using a dynamic Boolean network model combined with experimental validations using two isogenic human ovarian cancer cell lines that differ in their extracellular matrix-dependent migratory capacity. We found that cyclical bursts of RhoA activity are induced during cell migration, and that the negative feedbacks interconnecting Src, FAK, and/or CSK are critical for driving the cyclical RhoA activity. Disruption of the critical negative feedbacks by inhibiting CSK strongly suppressed cyclical bursts of RhoA activity and motility, implying that targeting these feedbacks is an effective strategy for interfering with cancer cell migration. Our findings also highlight the significance of network-level analyses for understanding complex bio-molecular regulatory mechanisms.

Results

Strategy for the reconstruction of the Rho-family GTPases signaling network model

Our aim was to understand how the activity of Rho-family GTPases is regulated at cell protrusions and correlate the biochemical events with extracellular matrix-dependent migration as biological network output. For this purpose, we first reconstructed a generic Rho-family GTPases signaling network by integrating all relevant information of individual key proteins, which we identified in the respective cell lines by mass spectrometry, and their interactions through an extensive survey of the literature (see Supplementary Materials and methods). This network includes signaling nodes from the Ras-ERK/PI3K cascade, as well as adhesion components operating downstream of the EGF receptor. A further layer of signaling nodes involves GEFs and GAPs that ultimately control the activity of the three canonical Rho GTPases: RhoA, Rac1, and Cdc42. This initial network is generic and does not include localization-specific spatial information. In order to derive a network that reflects Rho activation at leading edge protrusions, we (i) calibrated this network with experimental data measuring RhoA activity at protrusions, and (ii) refined the network topology that correctly simulates the experimentally observed RhoA activities through systematically eliminating network connections. This strategy allowed us to derive a network that accurately described changes in RhoA activity states at protrusions and could be used to analyze the signaling nodes that control these activities. Although not explicitly measured in a spatially resolved manner, the network also allows making predictions of the activities of Rac and Cdc42 GTPases.

Due to the generally very limited information on the kinetics of each biochemical interaction, continuous, differential equation-based models that model each biochemical reaction are difficult to parameterize realistically for large complex networks (Helikar et al., 2008). To avoid this problem, parameter-free discrete logic-based models have been applied to explore generic properties of complex bio-molecular regulatory networks (Gupta et al., 2007; Helikar et al., 2008; Kwon and Cho, 2008a, b; Saez-Rodriguez et al., 2009). Although these models simplify the kinetics of biochemical reaction to on-off relationships, they are still very useful to model global network states and assess dynamic changes as

methods). Only two attractors were observed in all the cases, labeled 1 and 2. Only the states of the Rho-family GTPases (i.e. RhoA, Rac, and Cdc42) in each attractor are shown for simplicity (see Supplementary Table S5 for all the states in the network for each attractor). The 'basin size' refers to the relative size of 'basin of attraction' given in percentage for each attractor. The 'Normal', 'A2780', and 'A2780-Rab25' denote 'intact mutation-free', 'inactive PTEN mutation', and 'inactive PTEN and active integrins mutation' conditions, respectively. (**C**) Sample activity maps (bottom panel) of RhoA, alongside with respective sampling windows (labeled 1–35; top panel) from similar regions of cells upon EGF stimulation. Scale bar, 5 μM. The color bar indicates the activation level of RhoA. Bursts of RhoA activities induced by EGF stimulation are visible in both A2780 (windows 20–35) and A2780-Rab25 (windows 15–25) cells. (**D**) EGF stimulation increases the average number of RhoA activity bursts in both A2780 and A2780-Rab25 cells. Error bars indicate standard error of the mean (SEM) of $n = 3–5$ cells per condition. (**E**) Migratory characteristics of A2780 and A2780-Rab25 cells on CDM in response to EGF. The average speeds of cells are increased in both A2780 and A2780-Rab25 cells, whereas the migration persistence is increased only in A2780-Rab25 cells upon EGF stimulation. Error bars indicate SEM of all cells ($n = 3$ biological replicates and at least 50 tracked cells per condition). A random sample of cell migration patterns, illustrated in form of stars, shows how EGF stimulation affects migration speed in comparison with starved condition (data from A2780 random cell migration). (**F**) Rac1 and Cdc42 activities induced by EGF stimulation in both A2780 and A2780-Rab25 cells detected by pulldown assays and western blotting.

Downloaded from https://academic.oup.com/jmcb/article/7/3/242/890313 by guest on 20 August 2022

transitions between these states. Therefore, we developed a discrete Boolean model based on the mechanistic information about the activation and/or inhibition of each signaling protein (see Supplementary Materials and methods and Table S4). In the Boolean network model, the state value of each node represents its activity, and is discretely represented as either '0' for an inactive or '1' for an active state.

The resulting generic literature-based signaling network consists of 33 nodes and 83 directed links (Figure 1A and Supplementary Table S2). This network contains an external-input node epidermal growth factor (EGF), which provides a potent extracellular cue for migration, and three output nodes for the best characterized Rho-family GTPases, i.e. RhoA, Rac, and Cdc42. The generic network is highly interconnected with at least 121 (62 negative and 59 positive) feedback loops such that any two nodes in the network are connected to each other, except for the external-input node EGF (see Supplementary Materials and methods and Table S3).

For the experimental validations, we used a well-established cellular model of extracellular matrix-dependent migration consisting of the human ovarian cancer cell line A2780, which has a loss-of-function mutation of PTEN, and its derivative A2780-Rab25, which overexpresses Rab25 (Cheng et al., 2004; Caswell et al., 2007). Rab25 has been linked to tumor progression, aggression, and metastasis, both clinically and in mouse models (Cheng et al., 2004). Rab25 enhances extracellular matrix-dependent migration by delivering integrins to the plasma membrane at protrusions and increasing migration persistence (Caswell et al., 2007). This increases the ability of cancer cells to invade the extracellular matrix. Hence, in our computational model, the cellular contexts of A2780 and A2780-Rab25 are represented by introducing constitutively inactive PTEN without and with constitutively active integrins, respectively. Interestingly, when these cells are plated on plastic, i.e. without integrin engagement, Rab25 overexpression does not alter cell morphology or cell migratory characteristics, such as velocity, persistence, directionality, and formation of protrusions. On the other hand, when plated on a cell-derived matrix (CDM), a pseudo-3D environment produced by fibroblasts, Rab25 overexpression changes cell morphology and promotes extracellular matrix-dependent migration (Cukierman et al., 2001; Caswell et al., 2007). In order to keep the coherence of our computational modeling and experimental validation, we also used EGF as an external input in both cell lines. As we were specifically interested in extracellular matrix-dependent migration, we characterized and experimentally measured this by the combination of random cell migration speed and persistence using cells plated on CDM under EGF-free and EGF stimulation conditions, making our results particularly relevant for EGF-induced and CDM-dependent migration.

Analysis of the generic Rho GTPase signaling network

The behavior of a complex cellular regulatory network can be effectively analyzed in a state-space where each point represents one network state defined by 'a set of state values containing the activity states of all signaling nodes in the network' (Huang et al., 2005; Bhattacharya et al., 2011; Ding and Wang, 2011; Choi et al., 2012). The network dynamics can be viewed in terms of a flow in the state-space that connects transition trajectories among all possible network states (Helikar and Rogers, 2009). Although protein activities are dynamically regulated by interactions among many signaling proteins in the network, they will eventually reach certain characteristic stable states called 'attractors' (Choi et al., 2012). Depending on whether the attractor consists of a single network state or a set of network states forming a cycle, it is classified as a point attractor or a cyclic attractor. The region of network states around a particular attractor with trajectories converging toward the attractor is called the 'basin of attraction' (Huang et al., 2005).

We applied this state-space approach to our generic Rho-family GTPases signaling network, in which an attractor represents a stable state of protein activities. The attractors are identified from Boolean simulations using randomly sampled initial conditions or network states (see Supplementary Materials and methods). Although various attractors can be present in the state-space, cellular behavior is often governed by the dominant stable state known as a 'primary attractor' with the largest basin of attraction (Li et al., 2004). We simulated the behavior of Rho-family GTPases in three network contexts, (i) a normal, mutation-free network, (ii) a PTEN-mutated network reflecting the A2780 cells, and (iii) a network with PTEN mutation and activated integrins representing the A2780-Rab25 cells. Under EGF-free conditions, the majority of network states eventually converged into primary point attractors where all the Rho-family GTPases were inactive (left panel in Figure 1B and top panel in Supplementary Figure S1). When EGF stimulation was applied, cyclic attractors appeared (right panel in Figure 1B and bottom panel in Supplementary Figure S1), i.e. the network converged on recursive cycling between network states. Specifically, RhoA and Rac were cyclically activated in both primary and secondary attractors for all three cellular contexts. In contrast, Cdc42 was cyclically activated only in the normal and A2780 contexts, but was persistently activated in the A2780-Rab25 context.

In accordance with our simulation results, bursts of RhoA activity at leading edge protrusions were induced by EGF in both A2780 and A2780-Rab25 cells as determined by FRET biosensor experiments (Figure 1C, Supplementary Videos S1 and S2). EGF also increased the average number of RhoA activity bursts (Figure 1D), and augmented the speed of migration on CDM in both A2780 cell lines (left panel in Figure 1E). However, EGF enhanced the persistence of migration only in A2780-Rab25 cells (right panel in Figure 1E). This property has previously been associated with a more invasive behavior of A2780-Rab25 cells compared with A2780 cells (Caswell et al., 2007). Rac and Cdc42 activity, determined by pulldown assays, was low in untreated cells, and inducible by EGF to similar extents in both cell lines (Figure 1F). Currently, Rac and Cdc42 FRET biosensors, which are GDI-regulated, are not robust enough to measure spatially resolved kinetics of Rac and Cdc42 activities on CDM in the number of living cells needed for statistically significant measurements. Thus, these experimental results show that all three Rho-family GTPases are activated by EGF, and that consistent with the model predictions, bursts of RhoA activity are induced by EGF in both cell lines (Figure 1B).

Downloaded from https://academic.oup.com/jmcb/article/7/3/242/890313 by guest on 20 August 2022

Identification of a critical signaling-feedback module that drives RhoA activity bursts at protrusions by network pruning

Having identified cyclical RhoA activation dynamics in computational simulations that might represent experimentally measured bursts of RhoA activity poses the question of the network-encoding source of such activities. Negative feedbacks have been shown to be capable of generating oscillations or cyclical behavior in many biological systems depending on the cellular context (Kholodenko, 2000; Wolkenhauer et al., 2004; Kwon and Cho, 2007; Goh et al., 2008; Tsai et al., 2008). It is important to note that our modeling strategy represents an abstraction that does not account for exact quantitative features, such as amplitude or oscillation frequencies, but can identify general regulatory roles of such feedback modules arising from the context of the network topology. Thus, the purpose of our model is to enable the network-based discovery of signaling modules that regulate Rho-family GTPases. The Rho-family GTPases signaling network comprises many negative feedbacks (Supplementary Table S3). In order to systematically identify critical negative feedbacks that drive the cyclical RhoA/Rac activities in the model (Figure 1B), we *in silico* deleted each link testing how effectively cyclical RhoA/Rac activities were suppressed by removal of a particular link under persistent EGF stimulation (Figure 2A). As RhoA activities were experimentally measured at protrusions, this *in silico* link deletion analysis effectively identified which links are relevant for controlling RhoA behavior at leading edge protrusions, enabling us to reconstruct the topology of the signaling network that controls RhoA activation at the leading edge. For each link deletion, the effectiveness of perturbation was measured by the remaining percentage of cases with cyclical activities in either RhoA or Rac for all initial network states (see Supplementary Materials and methods). The link deletions that disrupted cyclical RhoA/Rac activities $>1\%$ are shown in Figure 2A (see the figure legend for details). This analysis identified the negative-feedback modules in the network, which are perturbed by these link deletions, revealing a dynamic rewiring between the normal, A2780, and A2780-Rab25 networks (see Supplementary Materials and methods, Figure 2B–D).

More importantly, the link deletion analysis also identified core modules, which entertain cyclical activities in different cellular contexts. We found that 'CSK inhibiting (−|) Src', 'Src activating (→) CSK', 'FAK → CSK', and 'EGF → EGFR' links are critical for cyclical RhoA/Rac activities, since deletion of either link severely reduced (i.e. $<50\%$) the cyclical activities of both RhoA and Rac in all cellular contexts (Figure 2A). The 'EGF → EGFR' link is required for RhoA/Rac activation. The remaining critical links form a negative-feedback module, which includes two negative feedbacks composed of Src, FAK, and/or CSK that can generate cyclical activities: 'Src → CSK −| Src' and 'Src → FAK → CSK −| Src' (Figure 2E). As this is the only critical negative-feedback module that is common to all cellular contexts (indicated by dashed lines in Figure 2B–D), we suggest that the negative-feedback module composed of Src/FAK/CSK is an essential driver of cyclical RhoA/Rac activities in the pruned (i.e. protrusion-specific) model, and that disruption of this module might interfere with migration in all cellular contexts.

Notably, the effectiveness of perturbations for the common Src/FAK/CSK negative-feedback module was different depending on the cellular context: complete suppression of cyclical RhoA/Rac activities was only observed in the A2780-Rab25 context (Figure 2A). For the normal and A2780 contexts, there is another critical negative-feedback module consisting of 'EGFR → PTP_EGFR −| EGFR' (indicated by dotted lines in Figure 2B and C). Disruption of this feedback module resulted in the complete suppression of cyclical RhoA/Rac activities in the normal cellular context (Figure 2A), suggesting its dominance over Src/FAK/CSK module for cyclical RhoA/Rac activities. In the A2780 context, disruption of neither EGFR/PTP_EGFR nor Src/FAK/CSK module resulted in a complete suppression of cyclical RhoA/Rac activities. However, cyclical RhoA/Rac activities were entirely abolished by any combinatorial link deletion that disrupted both negative-feedback modules (Supplementary Figure S2), suggesting that they cooperate to generate cyclical activities for RhoA and Rac in the A2780 context. Therefore, the model predicts that essential negative-feedback modules required for cyclical RhoA/Rac activities might change as the cellular context changes, with normal cells requiring the EGFR/PTP_EGFR module, A2780-Rab25 requiring the Src/FAK/CSK module, and A2780 as an intermediate using both modules (Figure 2F).

Designing model-based intervention strategies for interfering with extracellular matrix-dependent cell migration

A major goal of the model analysis was to identify mechanisms for blocking extracellular matrix-dependent cell migration. Therefore, we systematically investigated strategies for disrupting the cyclical activities generated by the aforementioned negative-feedback modules. To this end, we performed *in silico* node control analysis under persistent EGF stimulus by pinning the state of each node to either '0' for complete inhibition or '1' for constitutive activation. The effectiveness of the node control was measured in the same manner as in the link deletion analysis, i.e. by determining the remaining percentage of cases with cyclical activities in either RhoA or Rac (see Supplementary Materials and methods). Only the results that disrupted cyclical activities are shown in Figure 3A.

Interestingly, the results of the node control analysis confirmed the significance of the Src/FAK/CSK and EGFR/PTP_EGFR negative-feedback modules in regulating RhoA and Rac activities. Persistent inhibition of CSK or activation of Src or FAK induced sustained RhoA activation and Rac inhibition leading to a severe suppression (i.e. $<40\%$; Figure 3A) of cyclical RhoA and Rac activities in all cellular contexts (Figure 3B). On the contrary, persistent inhibition of Src or FAK or activation of CSK was effective only in the A2780-Rab25 context, while RhoA and Rac were still cyclically activated in the normal and A2780 contexts (Figure 3B). Any perturbation of Src or CSK suppressed the cyclical activity of the Src/FAK/CSK module itself in the primary attractors of all cellular contexts. What causes this differential effect of the Src/FAK/CSK module on the regulation of cyclical RhoA/Rac activities? For Src=0 and CSK=1, the cyclical signal generated by the EGFR/PTP_EGFR module is still transmitted to downstream effectors through PI3K

Downloaded from https://academic.oup.com/jmcb/article/7/3/242/890313 by guest on 20 August 2022

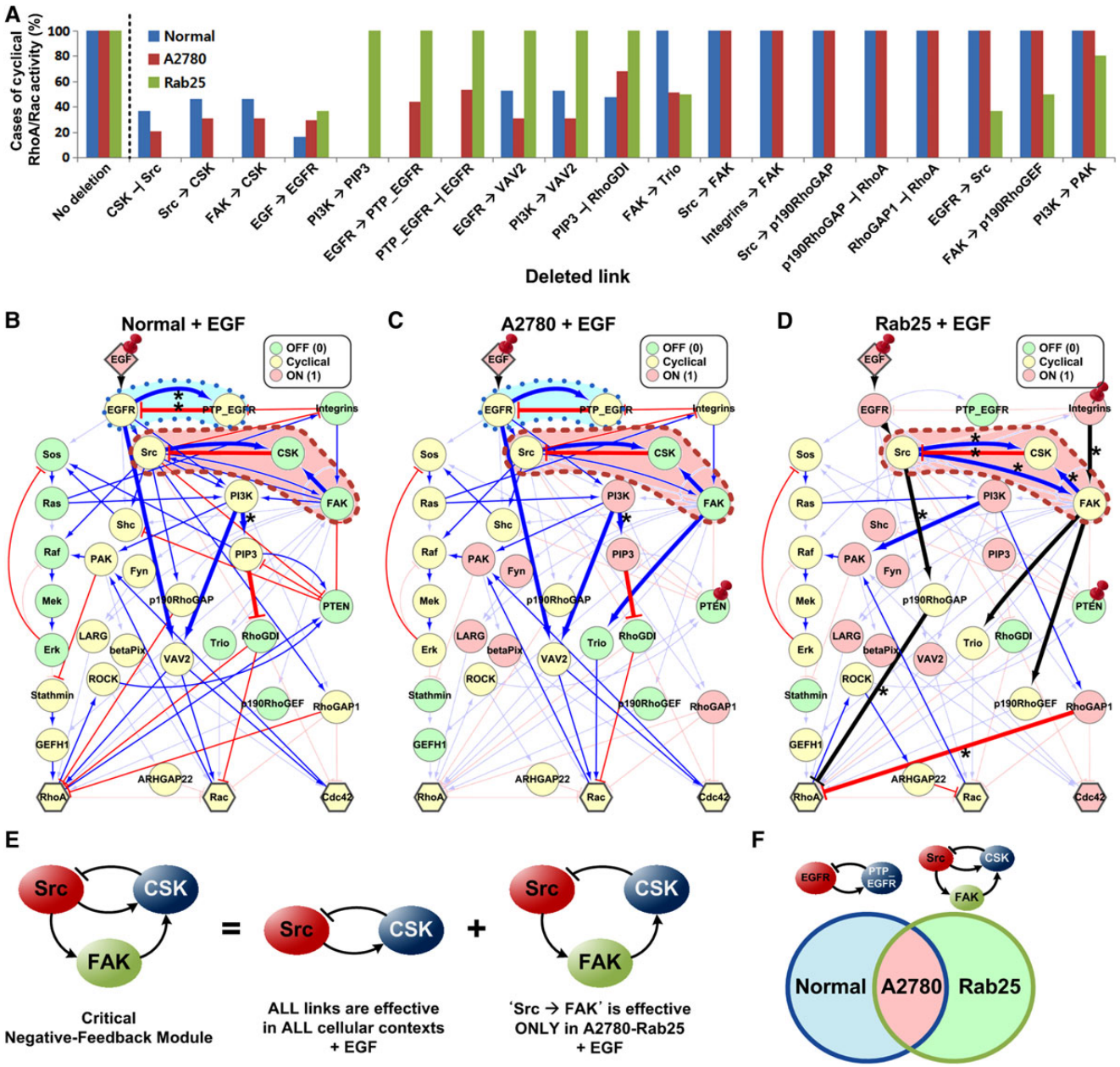

Figure 2 Identification of a critical negative-feedback module that regulates cyclical RhoA/Rac activities. (**A**) Link deletion analysis to identity links that interrupt cyclical activities in both RhoA and Rac. After deletion of each link, Boolean simulations were performed under persistent EGF. The effectiveness of each link deletion is represented by the remaining percentage of cases with cyclical activities in either RhoA or Rac from all 100000 cases of initial network states, when compared with 100% for the perturbation-free condition. Only the effective links (i.e. disruption of which resulted in <99% remaining cases with cyclical activities in either RhoA or Rac) are shown. The links 'CSK –| Src', 'Src → CSK', 'FAK → CSK', and 'EGF → EGFR' are critical for cyclical RhoA/Rac activities, since disruption of either results in strong inhibition (i.e. <50%) of both RhoA and Rac cyclical activities in all cellular contexts. (**B**–**D**) Negative-feedback network composed of the negative feedbacks that include at least one effective link for normal (**B**), A2780 (**C**), and A2780-Rab25 (**D**) contexts under persistent EGF stimulation. The critical negative-feedback module composed of Src, FAK, and CSK (encircled by a dashed line) is common to all cellular contexts under persistent EGF stimulation. Another negative-feedback module consisting of EGFR and PTP_EGFR (encircled by a dotted line) is also required for cyclical RhoA/Rac activities in the normal and A2780 contexts. The effective links shown in **A** are highlighted by thick lines, and the effective links that are not part of the corresponding effective negative-feedback network are colored black. Asterisks denote the essential links that result in a complete disruption of cyclical RhoA/Rac activities as shown in **A**. The color of each node represents its state in the primary attractor for each cellular context (i.e. green for 0 = off, yellow for cyclical activity, and red for 1 = on). (**E**) The critical negative-feedback module is composed of Src, FAK, and CSK. It contains three common effective links: 'CSK –| Src', 'Src → CSK', and 'FAK → CSK'. Two negative feedbacks are embedded in this module: 'Src → CSK –| Src' and 'Src → FAK → CSK –| Src'. Functionally, the two feedbacks are equivalent to a single system that incorporates both feedbacks. (**F**) The

Downloaded from https://academic.oup.com/jmcb/article/7/3/242/890313 by guest on 20 August 2022

in the normal and A2780 contexts, whereas Src=1 and CSK=0 conditions nullify the transfer of a cyclical signal by causing persistent PI3K activity (Supplementary Figure S3). In fact, the combined inhibition of Src with PI3K resulted in the complete suppression of RhoA/Rac cyclical activities in all cellular contexts (Supplementary Figure S4). Both EGFR=0 and PTP_EGFR=1 result in the EGFR being unresponsive to EGF, causing an effect similar to the deletion of the 'EGF → EGFR' link. In contrast, EGFR=1 and PTP_EGFR=0 are similar to disrupting the EGFR/PTP_EGFR negative-feedback module by deletion of either 'EGFR → PTP_EGFR' or 'PTP_EGFR –| EGFR' link (Figures 2A and 3A).

It is very reasonable to assume that a disruption of cyclical RhoA/Rac activities will stall the leading edge and consequently also forestall cell migration. In this respect, our modeling results suggested that EGF-induced and CDM-dependent migration might be effectively blocked by CSK inhibition through the disruption of both RhoA and Rac cyclical activities in all cellular contexts, whereas Src or FAK inhibition should be effective only in the A2780-Rab25 context (Figure 3B). In order to validate this simulation-derived hypothesis, a specific Src-family kinase inhibitor (PP2) and CSK siRNA were used for perturbing the system. Currently, FAK small-molecule inhibitors are less specific. Therefore, we did not include them in our validation. Consistent with our hypothesis, the Src inhibitor disrupted cyclical bursts of RhoA activity (top panel in Figure 3C, Supplementary Videos S1 and S2), decreased the average number of RhoA activity bursts (Figure 3D), and impeded the migration speed (Figure 3E) only in A2780-Rab25 cells. On the other hand, knocking down CSK was inhibitory to all these outputs in both cell lines (Figure 3D, bottom panel in Figure 3C, Supplementary Videos S1 and S2). Both migration speed and persistence were decreased by CSK knockdown in A2780-Rab25 cells, indicating reduced overall migration, but only a severe reduction in migration speed was observed in A2780 cells without any change in persistence, leading to the decrease in the overall migration (Figure 3E). Moreover, although the Src inhibitor failed to impede the migration speed in A2780 cells, the combinatorial inhibition of Src and PI3K (one of the direct effectors of EGFR) synergistically reduced the migration speed and persistence further and even below those of starved cells (Figure 3F). Notably, either Src or CSK inhibition reverted the increased migration persistence by EGF in A2780-Rab25 cells back to the level seen in starved cells (Figure 3E). These results show that Src and surprisingly also CSK inhibition can interfere with cell migration. Src inhibition blocks cyclical RhoA activity and migration in the A2780-Rab25 cells, where EGF-induced and CDM-dependent migration is enabled by enhanced integrin delivery to the cell membrane (Caswell et al., 2007), but is ineffective in A2780 cells where migration is promoted by PTEN mutation (Wu et al., 2008). On the other hand, CSK inhibition could interfere with cyclical RhoA activation and cell migration in both A2780 and A2780-Rab25 cells, suggesting that the effects of Src inhibition on cancer cell migration are more context-dependent than the effects of CSK.

Discussion

In summary, our data suggest that when cells are stimulated to migrate by application of EGF, the negative-feedback modules Src/FAK/CSK and/or EGFR/PTP_EGFR generate the signals that drive the cyclical RhoA/Rac activities, which are required for cell migration (Figure 4A and B). The cyclical RhoA/Rac activities have been suggested to coordinate the cycles of membrane protrusion and retraction that enable cells to migrate (Machacek et al., 2009). It was experimentally found that the global motile behavior of podosome-like structure (PLS) zones results from the cycles of single PLS appearance/disappearance (Martin et al., 2014). The formation of a PLS zone was dynamically correlated with low RhoA and myosin activity at the leading edge (Martin et al., 2014). In addition, the motility of the cells expressing constitutively active RhoA mutant (RhoA-V14) was dramatically reduced, consistent with the hypothesis that high RhoA activity suppresses motility by preventing Rac-induced protrusions (Vial et al., 2003). Increased RhoA activity might be the cause of increased stress fiber formation and focal adhesions, which in turn inhibits protrusions, polarized phenotype, and cell motility (Vial et al., 2003). Together, these suggest that cyclical bursts of RhoA activity are needed at the protrusion site for cell migration. The cyclic RhoA activity, which in turn negatively feeds back to FAK through PTEN (Figure 1A), might contribute to the oscillatory FAK and Src activity, causing an iterative adhesion assembly and disassembly, and providing a necessary push-pull mechanism for the cells to move forward.

Any interruption of the cyclical activities of the Rho-family GTPases, such as the CSK inhibition as presented in this study, might lead to an effective therapeutic strategy for interfering cancer cell migration. This result may seem counterintuitive, as Src has been shown to stimulate cell migration and invasiveness (Guarino, 2010), and CSK inhibits Src (Ia et al., 2010). However, as the modeling and experimental work shows, the salient principle of inhibiting migration is to break the cyclically bursting activities of RhoA, and also possibly Rac as shown from simulations. Thus, targeting specific dynamic properties of signal transduction networks rather than a node itself may constitute a promising principle that expands the space of potential drug targets. From this point of view, it is plausible that inhibition of either Src or CSK can block migration. Previous work showed that downregulation of CSK can activate Src and enhance cell migration (Vidal and Cagan, 2006; Liang et al., 2007). These results are not necessarily in conflict with ours, as we show that the effects of Src or CSK inhibition are dependent on the cell context. Alternatively, these discrepancies may be due to the use of different model systems, i.e. *Drosophila*

usage of essential feedback modules shifts depending on cellular contexts. The critical negative-feedback module interconnecting Src, FAK, and CSK is essential in the A2780-Rab25 context, since any link disruption results in complete suppression of cyclical RhoA/Rac activities. On the other hand, only the EGFR/PTP_EGFR negative-feedback module is essential in the normal cellular context, whereas disruption of both modules is required for entire suppression of cyclical RhoA/Rac activities in A2780 context.

Downloaded from https://academic.oup.com/jmcb/article/7/3/242/890313 by guest on 20 August 2022

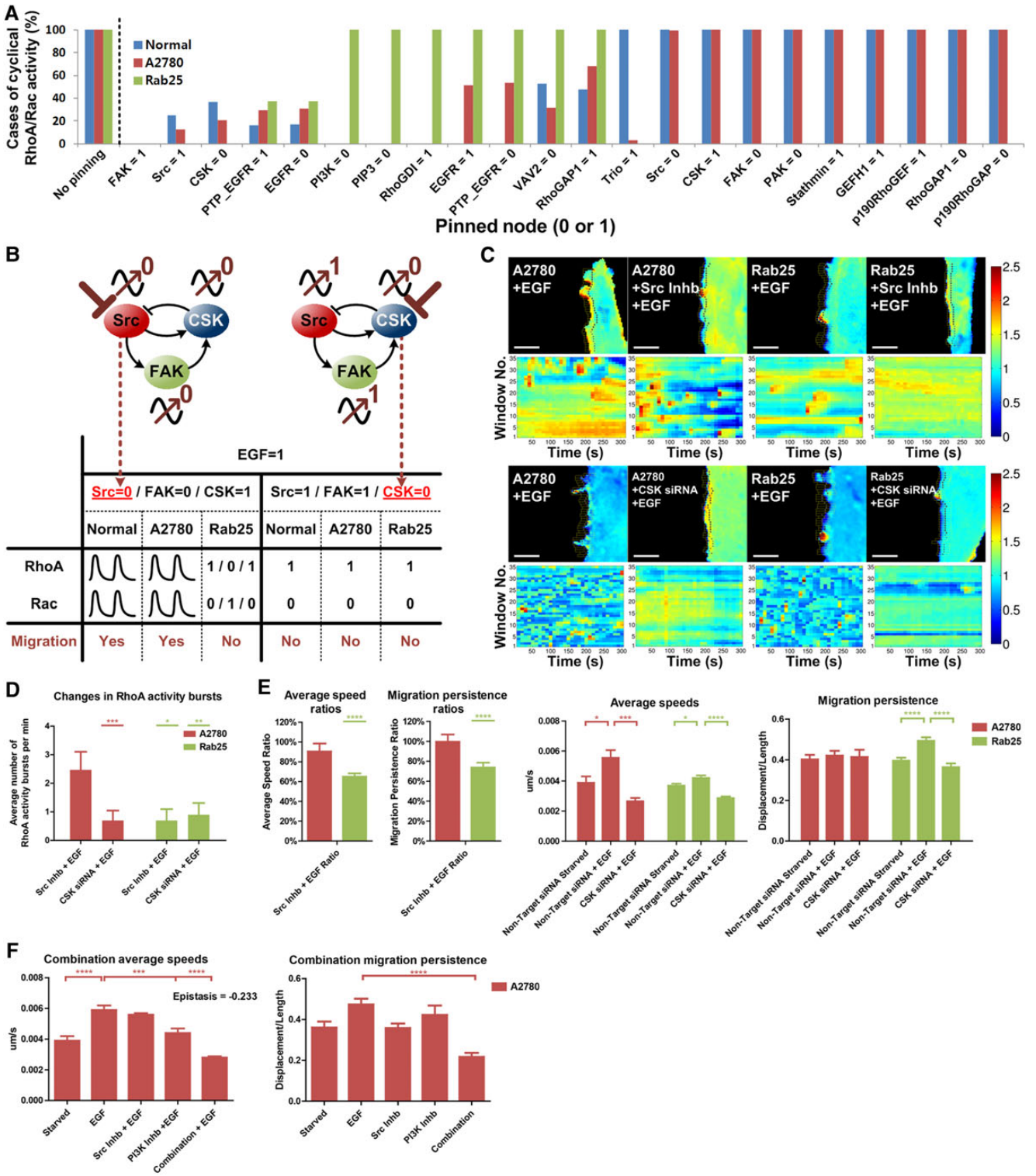

Figure 3 Designing interventions that block extracellular matrix-dependent cell migration. (**A**) Node control analysis for the effective disruption of cyclical RhoA/Rac activities. Each node was pinned to either '0' or '1' before Boolean simulations were performed under persistent EGF stimulation. The effectiveness of perturbation is measured in the same way as in the link deletion analysis. The persistent inhibition of CSK or activation of Src or FAK results in the strong suppression (i.e. $<40\%$) of both RhoA and Rac cyclical activities in all cellular contexts. In contrast, the persistent inhibition of Src or FAK or activation of CSK is effective only in A2780-Rab25. (**B**) Contrasting node control effects for the complete inhibition or constitutive activation of Src, FAK, or CSK. Although persistent inhibition of Src also suppresses FAK and CSK, the cyclical RhoA/Rac activities still remain undisrupted in the normal and A2780 contexts. (**C**) Sample activity maps (second and fourth rows) of RhoA, alongside with respective sampling

Downloaded from https://academic.oup.com/jmcb/article/7/3/242/890313 by guest on 20 August 2022

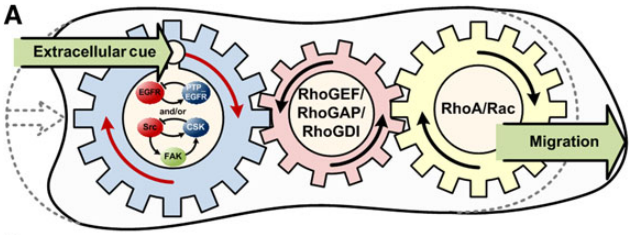

B

Cell Type	Integrins	EGF	RhoA/Rac	Migration	Invasiveness
A2780	–	0	———	No	No
	–	1	∧∧	Yes	Low
A2780-Rab25	1	0	———	No	No
	1	1	∧∧	Yes	High

Figure 4 The underlying regulatory mechanism for cell migration. (**A**) Upon an extracellular cue for migration, the negative-feedback modules Src/FAK/CSK and/or EGFR/PTP_EGFR generate the cyclical signal. This signal drives the cyclical RhoA/Rac activities through the regulation of Rho-GEFs, Rho-GAPs, and Rho-GDIs, thereby modulating the cell migration by inducing iterative cyclic events of protrusions and retractions. (**B**) The relationship between RhoA/Rac activity and cell migration for A2780 and A2780-Rab25. The cyclical RhoA/Rac activities are required for cell migration, and the invasiveness of migrating cells might be relative to the persistence of migration as observed by the enhanced migration persistence of A2780-Rab25 cells by EGF (right panel in Figure 1E).

(Vidal and Cagan, 2006), or different assays for cell migration (Liang et al., 2007).

Interestingly, perturbations within the Src/FAK/CSK negative-feedback module showed different effects depending on the genetic background of the cells. Inhibition of Src blocked cyclical bursts of RhoA activity and migration only in the EGF-induced and CDM-dependent migratory (A2780-Rab25) cells, whereas CSK downregulation efficiently inhibited both processes in the EGF-induced and CDM-dependent migratory and parental (A2780) cancer cells. Importantly, these results suggest that CSK inhibition can prevent cancer cells from becoming migratory and invasive, while Src inhibition can only block migration of cancer cells that already have acquired an EGF-induced and CDM-dependent migratory phenotype.

For metastasis, cancer cells need to acquire both motility and invasive capacity. As supported by the enhanced migration persistence of A2780-Rab25 cells by EGF (right panel in Figure 1E) and the persistently active Cdc42 in our simulations (right bottom panel in Figure 1B), the migration persistence might affect the invasiveness of migrating cells (Figure 4B) by potentiating the directionality of movement possibly through Cdc42 (Sahai and Marshall, 2002). Hence, our Rho-family GTPases signaling network model may further be extended and utilized to investigate the invasive capacity conferred to cancer cells by Rac and Cdc42. Intriguingly, tumor cells may switch between mutually exclusive modes of invasion, depending on the microenvironment they encounter as they move away from the primary tumor: (i) a Rac-dependent, mesenchymal type of invasion with elongated morphology, and (ii) a RhoA-dependent, amoeboid type of invasion with rounded morphology (Croft and Olson, 2008). Furthermore, it will be also interesting to integrate the migration model with other cellular functions of the Rho-family GTPases, such as cell polarization and cell cycle regulation (Sahai and Marshall, 2002), for the study of overall coordination between cell movement and cell proliferation that contribute to metastatic tumor growth.

Cells are composed of numerous molecular components that are interacting with each other and form a complex molecular interaction network. Therefore, to have a proper understanding of the functional role of each molecular component, we need to investigate the regulatory relationship of the component within the context of the whole interaction network. Recent technological developments opened up various 'omics' studies, leading to a paradigm shift in disease diagnosis and treatment (Marko and Weil, 2010; Barretina et al., 2012; Hoadley et al., 2014). Molecular sub-typing of colorectal cancer for more effective treatment is one of the examples (De Sousa et al., 2013; Sadanandam et al., 2013). However, even if we can identify drug targets

windows (first and third rows) from similar regions of cells in different conditions. Scale bar, 5 μm. The color bar indicates the activation level of RhoA. While Src inhibition has no effect on the cyclical bursts of RhoA activity in A2780 (windows 25–35 for EGF and 10–20 for Src inhibition), it disrupts the cyclical bursts of RhoA activity induced by EGF stimulation (windows 10–25) only in A2780-Rab25 cells (no visible activity bursts). CSK knockdown disrupts the cyclical bursts of RhoA activity induced by EGF stimulation (windows 1–15 for A2780 and 5–20 for A2780-Rab25) in both cell lines (no visible activity bursts). (**D**) The differential effect of Src inhibition and CSK knockdown on the average number of RhoA activity bursts, induced by EGF stimulation (refer to Figure 1**D**) in A2780 and A2780-Rab25 cells. Src inhibition decreases the average number of RhoA activity bursts only in A2780-Rab25 cells, whereas CSK knockdown decreases the average number of RhoA activity bursts in both A2780 and A2780-Rab25 cells. (**E**) The differential effects of Src inhibition (left two panels) and CSK knockdown (right two panels) on the migratory characteristics of A2780 and A2780-Rab25 cells. Average speed and migration persistence ratios are calculated by normalizing the respective values to their EGF-treated counterparts. Src inhibition decreases both average migration speed and persistence only in A2780-Rab25 cells. CSK knockdown decreases average migration speeds in both A2780 and A2780-Rab25 cells, although it only decreases the migration persistence of A2780-Rab25 cells. (**F**) Migratory behavior of A2780 cells in response to combined inhibition of Src and PI3K. Combined inhibition of Src and PI3K (using PP2 and/or LY294002 at 10 μM) synergistically reduces the migration speed of A2780 cells. The epistasis index is calculated based on the non-scaled epistasis definition (Segre et al., 2005) by normalizing all values to EGF values and predicting the additive effect of the two inhibitions. The calculated epistasis index of −0.233 shows that combinatorial inhibition of Src and PI3K is 23.3% more effective than the addition of the effects of the separate inhibitions. For **D–F**, error bars indicate SEM of all cells ($n = 3$ biological replicates and at least 50 tracked cells per condition).

Downloaded from https://academic.oup.com/jmcb/article/7/3/242/890313 by guest on 20 August 2022

through statistical analysis, the underlying mechanisms involved still remain elusive. The modeling approach can be useful for unraveling the hidden design principle in the underlying complex molecular interaction network by systematically analyzing the network dynamics using computer simulation (Choi et al., 2012; Shin et al., 2014). It can also be used to develop novel therapeutic strategies that overcome drug resistance (Lee et al., 2012; Won et al., 2012). The proposed network modeling approach based on attractor landscape analysis can be applied to any other complex molecular interaction network to get a new insight into the underlying regulatory mechanism and identify new drug targets.

Materials and methods

Rac1 and Cdc42 activation assay

Cells were lysed in ice-cold lysis buffer (50 mM Tris·Cl, pH 7.2, 1% (*w*/*v*) Triton X-100, 500 mM NaCl, 10 mM $MgCl_2$) supplemented with protease inhibitor PMSF (1 mM). Cleared lysates were incubated with 10 μg of GST-PAK-CRIB beads for 30 min at 4°C under end-to-end rotation. The beads were washed with wash buffer (50 mM Tris·Cl, pH 7.2, 1% (*w*/*v*) Triton X-100, 150 mM NaCl, 10 mM $MgCl_2$) supplemented with protease inhibitor PMSF (1 mM). The beads were re-suspended alongside with the total lysate, boiled in LDS Sample Buffer containing dithiothreitol (100 mM), and western blotted. Anti-Rac1 antibody (Millipore, clone 238A, 1:500) and anti-Cdc42 antibody (Santa Cruz Biotechnology, sc-87, 1:500) were used to detect both total and active Rac1 or Cdc42. The western blot bands were quantified using ImageJ.

Live cell migration

Random cell migration assays were performed on cell lines stably transduced with H2B-mRFP. Cells were seeded on CDM-coated plastic plates and images were captured every 10 min using fluorescence microscopy (excitation: 540 nm, emission: 588 nm) with an A-Plan 10×/0.25 ph1 objective, over a 12-h period. Movies were analyzed using Bitplane Imaris (version 7.6.4) spot detection and tracking module, and the average speeds and migration persistence of cells were calculated using MATLAB® software. Average speeds of cells were calculated by averaging the average frame-to-frame speed of all cells. Migration persistence was calculated by averaging the migration persistence of all the cells. The migration persistence of each cell is the total displacement divided by the total track length of the cell. All migration experiments were performed in triplicates, with at least 50 tracked cells per condition.

RhoA activity assessed by FRET imaging

The RhoA biosensor was imaged in live cells as previously described (Hodgson et al., 2010). Cells were seeded on CDM-coated glass-bottom plates. The biosensor-expressing cells were imaged at 10-sec intervals, using a Nikon Plan Apo 40×/1.5 DIC oil objective on a spinning-disk laser confocal Nikon microscope with Andor iXon^{EM+} EMCCD camera, using 4 averaged frames and no binning, resulting in an effective pixel size of 234 nm. The same excitation wavelength (445 nm) was used for both mTFP and FRET channels, while 475 and 526 nm emission filters were used for mTFP and FRET channels, respectively. Both mTFP and FRET channels were captured at ∼75% of camera overexposure using the same level of laser power (exposure time between 800–1000 msec for mTFP and 300–400 msec for FRET channel). Twenty images from a cell-free area using the same settings were also acquired for shading correction. The raw images were de-noised with the ImageJ PureDenoise plugin (Luisier et al., 2010), and then were analyzed with the Biosensor Processing Software 2.1 for MATLAB® from the Danuser Lab (Hodgson et al., 2010), using the default configuration. The processed biosensor images were normalized and compared by segmenting (35 windows) similar regions of boundaries of the cell using ImageJ and plotting the average RhoA activity over time of each window onto an activity map using MATLAB®. In order to compare different conditions quantitatively, all bursts of RhoA activities that were followed by a protrusion were considered and manually counted in all cells ($n = 3–5$) for each condition, then averaged and plotted.

Reconstruction and analysis of the Rho-family GTPases signaling network; cell lines and reagents; generation of cell-derived matrix; CSK siRNA knockdown

The details are described in the Supplementary Materials and methods.

Statistical analysis

The significance of differences in RhoA activity burst counts, migration speed, and persistence was measured using unpaired two-tailed Student's *t*-test.

Supplementary material

Supplementary material is available at *Journal of Molecular Cell Biology* online.

Funding

This work was supported by the National Research Foundation of Korea (NRF) grants funded by the Korea Government, the Ministry of Science, ICT and Future Planning (2014R1A2A1A10052404 and 2013M3A9A7046303) and by the KAIST Future Systems Healthcare Project from the Ministry of Science, ICT and Future Planning. This work was also supported by the Science Foundation Ireland under Grant No. 06/CE/B1129 and Walton Fellowship No. 11/W.1/B2075 to K.-H.C.

Conflict of interest: none declared.

References

Barretina, J., Caponigro, G., Stransky, N., et al. (2012). The Cancer Cell Line Encyclopedia enables predictive modelling of anticancer drug sensitivity. Nature *483*, 603–607.

Bhattacharya, S., Zhang, Q., and Andersen, M.E. (2011). A deterministic map of Waddington's epigenetic landscape for cell fate specification. BMC Syst. Biol. *5*, 85.

Burridge, K., and Wennerberg, K. (2004). Rho and Rac take center stage. Cell *116*, 167–179.

Caswell, P.T., Spence, H.J., Parsons, M., et al. (2007). Rab25 associates with α5β1 integrin to promote invasive migration in 3D microenvironments. Dev. Cell *13*, 496–510.

Downloaded from https://academic.oup.com/jmcb/article/7/3/242/890313 by guest on 20 August 2022

Cheng, K.W., Lahad, J.P., Kuo, W.L., et al. (2004). The RAB25 small GTPase determines aggressiveness of ovarian and breast cancers. Nat. Med. *10*, 1251–1256.

Choi, M., Shi, J., Jung, S.H., et al. (2012). Attractor landscape analysis reveals feedback loops in the p53 network that control the cellular response to DNA damage. Sci. Signal. *5*, ra83.

Croft, D.R., and Olson, M.F. (2008). Regulating the conversion between rounded and elongated modes of cancer cell movement. Cancer Cell *14*, 349–351.

Cukierman, E., Pankov, R., Stevens, D.R., et al. (2001). Taking cell-matrix adhesions to the third dimension. Science *294*, 1708–1712.

De Sousa, E.M.F., Wang, X., Jansen, M., et al. (2013). Poor-prognosis colon cancer is defined by a molecularly distinct subtype and develops from serrated precursor lesions. Nat. Med. *19*, 614–618.

Ding, S., and Wang, W. (2011). Recipes and mechanisms of cellular reprogramming: a case study on budding yeast Saccharomyces cerevisiae. BMC Syst. Biol. *5*, 50.

Friedl, P., and Wolf, K. (2010). Plasticity of cell migration: a multiscale tuning model. J. Cell Biol. *188*, 11–19.

Goh, K.I., Kahng, B., and Cho, K.H. (2008). Sustained oscillations in extended genetic oscillatory systems. Biophys. J. *94*, 4270–4276.

Guarino, M. (2010). Src signaling in cancer invasion. J. Cell. Physiol. *223*, 14–26.

Gupta, S., Bisht, S.S., Kukreti, R., et al. (2007). Boolean network analysis of a neurotransmitter signaling pathway. J. Theor. Biol. *244*, 463–469.

Hanahan, D., and Weinberg, R.A. (2000). The hallmarks of cancer. Cell *100*, 57–70.

Heasman, S.J., and Ridley, A.J. (2008). Mammalian Rho GTPases: new insights into their functions from in vivo studies. Nat. Rev. Mol. Cell Biol. *9*, 690–701.

Helikar, T., and Rogers, J.A. (2009). ChemChains: a platform for simulation and analysis of biochemical networks aimed to laboratory scientists. BMC Syst. Biol. *3*, 58.

Helikar, T., Konvalina, J., Heidel, J., et al. (2008). Emergent decision-making in biological signal transduction networks. Proc. Natl Acad. Sci. USA *105*, 1913–1918.

Hoadley, K.A., Yau, C., Wolf, D.M., et al. (2014). Multiplatform analysis of 12 cancer types reveals molecular classification within and across tissues of origin. Cell *158*, 929–944.

Hodgson, L., Shen, F., and Hahn, K. (2010). Biosensors for characterizing the dynamics of rho family GTPases in living cells. Curr. Protoc. Cell Biol. *46*, 14.11.1–14.11.26.

Huang, S., Eichler, G., Bar-Yam, Y., et al. (2005). Cell fates as high-dimensional attractor states of a complex gene regulatory network. Phys. Rev. Lett. *94*, 128701.

Huang, C.H., Tang, M., Shi, C., et al. (2013). An excitable signal integrator couples to an idling cytoskeletal oscillator to drive cell migration. Nat. Cell Biol. *15*, 1307–1316.

Ia, K.K., Mills, R.D., Hossain, M.I., et al. (2010). Structural elements and allosteric mechanisms governing regulation and catalysis of CSK-family kinases and their inhibition of Src-family kinases. Growth Factors *28*, 329–350.

Kholodenko, B.N. (2000). Negative feedback and ultrasensitivity can bring about oscillations in the mitogen-activated protein kinase cascades. Eur. J. Biochem. *267*, 1583–1588.

Kwon, Y.K., and Cho, K.H. (2007). Boolean dynamics of biological networks with multiple coupled feedback loops. Biophys. J. *92*, 2975–2981.

Kwon, Y.K., and Cho, K.H. (2008a). Coherent coupling of feedback loops: a design principle of cell signaling networks. Bioinformatics *24*, 1926–1932.

Kwon, Y.K., and Cho, K.H. (2008b). Quantitative analysis of robustness and fragility in biological networks based on feedback dynamics. Bioinformatics *24*, 987–994.

Lammermann, T., and Sixt, M. (2009). Mechanical modes of 'amoeboid' cell migration. Curr. Opin. Cell Biol. *21*, 636–644.

Lauffenburger, D.A., and Horwitz, A.F. (1996). Cell migration: a physically integrated molecular process. Cell *84*, 359–369.

Lee, M.J., Ye, A.S., Gardino, A.K., et al. (2012). Sequential application of anticancer drugs enhances cell death by rewiring apoptotic signaling networks. Cell *149*, 780–794.

Li, F., Long, T., Lu, Y., et al. (2004). The yeast cell-cycle network is robustly designed. Proc. Natl Acad. Sci. USA *101*, 4781–4786.

Liang, F., Liang, J., Wang, W.Q., et al. (2007). PRL3 promotes cell invasion and proliferation by down-regulation of Csk leading to Src activation. J. Biol. Chem. *282*, 5413–5419.

Luisier, F., Vonesch, C., Blu, T., et al. (2010). Fast interscale wavelet denoising of Poisson-corrupted images. Signal Process. *90*, 415–427.

Machacek, M., Hodgson, L., Welch, C., et al. (2009). Coordination of Rho GTPase activities during cell protrusion. Nature *461*, 99–103.

Marko, N.F., and Weil, R.J. (2010). Mathematical modeling of molecular data in translational medicine: theoretical considerations. Sci. Transl. Med. *2*, 56rv54.

Martin, K., Vilela, M., Jeon, N.L., et al. (2014). A growth factor-induced, spatially organizing cytoskeletal module enables rapid and persistent fibroblast migration. Dev. Cell *30*, 701–716.

Pertz, O., Hodgson, L., Klemke, R.L., et al. (2006). Spatiotemporal dynamics of RhoA activity in migrating cells. Nature *440*, 1069–1072.

Sadanandam, A., Lyssiotis, C.A., Homicsko, K., et al. (2013). A colorectal cancer classification system that associates cellular phenotype and responses to therapy. Nat. Med. *19*, 619–625.

Saez-Rodriguez, J., Alexopoulos, L.G., Epperlein, J., et al. (2009). Discrete logic modelling as a means to link protein signalling networks with functional analysis of mammalian signal transduction. Mol. Syst. Biol. *5*, 331.

Sahai, E., and Marshall, C.J. (2002). RHO-GTPases and cancer. Nat. Rev. Cancer *2*, 133–142.

Sander, E.E., ten Klooster, J.P., van Delft, S., et al. (1999). Rac downregulates Rho activity: reciprocal balance between both GTPases determines cellular morphology and migratory behavior. J. Cell Biol. *147*, 1009–1022.

Sanz-Moreno, V., Gadea, G., Ahn, J., et al. (2008). Rac activation and inactivation control plasticity of tumor cell movement. Cell *135*, 510–523.

Segre, D., Deluna, A., Church, G.M., et al. (2005). Modular epistasis in yeast metabolism. Nat. Genet. *37*, 77–83.

Shin, D., Kim, I.S., Lee, J.M., et al. (2014). The hidden switches underlying RORα-mediated circuits that critically regulate uncontrolled cell proliferation. J. Mol. Cell Biol. *6*, 338–348.

Tomar, A., and Schlaepfer, D.D. (2009). Focal adhesion kinase: switching between GAPs and GEFs in the regulation of cell motility. Curr. Opin. Cell Biol. *21*, 676–683.

Tsai, T.Y., Choi, Y.S., Ma, W., et al. (2008). Robust, tunable biological oscillations from interlinked positive and negative feedback loops. Science *321*, 126–129.

Tsyganov, M.A., Kolch, W., and Kholodenko, B.N. (2012). The topology design principles that determine the spatiotemporal dynamics of G-protein cascades. Mol. Biosyst. *8*, 730–743.

Vial, E., Sahai, E., and Marshall, C.J. (2003). ERK-MAPK signaling coordinately regulates activity of Rac1 and RhoA for tumor cell motility. Cancer Cell *4*, 67–79.

Vidal, M., and Cagan, R.L. (2006). Drosophila models for cancer research. Curr. Opin. Genet. Dev. *16*, 10–16.

Wolkenhauer, O., Ghosh, B.K., and Cho, K.H. (2004). Control and coordination in biochemical networks. IEEE Control Syst. Mag. *24*, 30–34.

Won, J.K., Yang, H.W., Shin, S.Y., et al. (2012). The crossregulation between ERK and PI3K signaling pathways determines the tumoricidal efficacy of MEK inhibitor. J. Mol. Cell Biol. *4*, 153–163.

Wu, H., Wang, S., Weng, D., et al. (2008). Reversal of the malignant phenotype of ovarian cancer A2780 cells through transfection with wild-type PTEN gene. Cancer Lett. *271*, 205–214.

Downloaded from https://academic.oup.com/jmcb/article/7/3/242/890313 by guest on 20 August 2022